Heterofullerenes: Structure and property predictions, possible uses and synthesis proposals

Heinrich R. Karfunkel[a],*, Thomas Dressler[b] and Andreas Hirsch[c]

aCiba-Geigy AG, KB-IT, R-1008.823, CH-4002 Basel, Switzerland
bIBM Germany, W-7000 Stuttgart 80, Germany
cUniversity of Tübingen, Auf der Morgenstelle 18, W-7400 Tübingen, Germany

SUMMARY

Substituting carbon atoms of fullerenes by heteroatoms and vacancies will lead to new and yet unknown spherical-shaped molecules termed hereafter as heterofullerenes. The enormous structural diversity of these molecules is investigated and their structural, electronic and thermochemical properties are predicted using semiempirical computations. Computational results for complexes with ions lead to the hypothesis that these molecules behave like microscopic Faraday cages in which the electrons concentrate on the outer side of the sphere. It is predicted that some of these heterofullerenes are structurally and electronically similar to phthalocyanines and related molecules but offer many additional advantages. Potential uses such as adding heterofullerenes to fullerene materials, as superior starting materials for the fabrication of diamonds, as catalysts in hydrogenation reactions, as components of materials dominated until now by phthalocyanines, etc., are discussed. Simple synthetic routes to these compounds that are based on minor alternations of existing methods for fullerene production are proposed. On the basis of the thermochemical calculations, we believe that the most promising possibility consists of using metal cyanide/graphite composite target rods instead of pure graphite rods as in a conventional fullerene synthesis.

INTRODUCTION

Fullerenes have attracted considerable interest since their discovery in 1985 by Kroto et al. [1]. A compact review of the work in this field (till 1991) is given by Kroto et al. [2]. The spectacular discoveries of outstanding physical and chemical properties such as conductivity, superconductivity, magnetism, non-linear optical properties and selective chemical reactivity [3–9] are direct-

---

* To whom correspondence should be addressed.

ing the interest of more and more scientists toward fullerene chemistry. The structural diversity of the higher fullerenes, such as C_{78} [10,11], and the myriad of products resulting from nucleophilic and radical addition reactions [6–9] are already very impressive. However, fullerene chemistry is restricted to fullerene skeletons containing only carbon atoms. Fullerenes containing heteroatoms in the basic skeleton (i.e., heteroatoms not resulting from addition reactions), such as $C_{59}B$ or $C_{58}B_2$ [12], are the exception rather than the rule. The increase in chemical diversity due to substitutions of basic skeleton carbons by heteroatoms could be compared to the increase related to the transition from aromatic hydrocarbons to heterocyclics.

In this article we present some of these hypothetical 'heterofullerenes' and predict their electronic properties, thermochemical properties and behavior by using semiempirical MNDO type calculations, which reveal that there are indeed no reasons to exclude their existence. Above all, we propose some minor variations to the experimental conditions under which the common fullerenes are synthesized which, we believe, will lead to some of these hypothetical molecules. We also indicate new potential uses of some of these molecules in research areas such as material sciences and supra-molecular chemistry, areas that were until now dominated by phthalocyanines, crown molecules and related compounds.
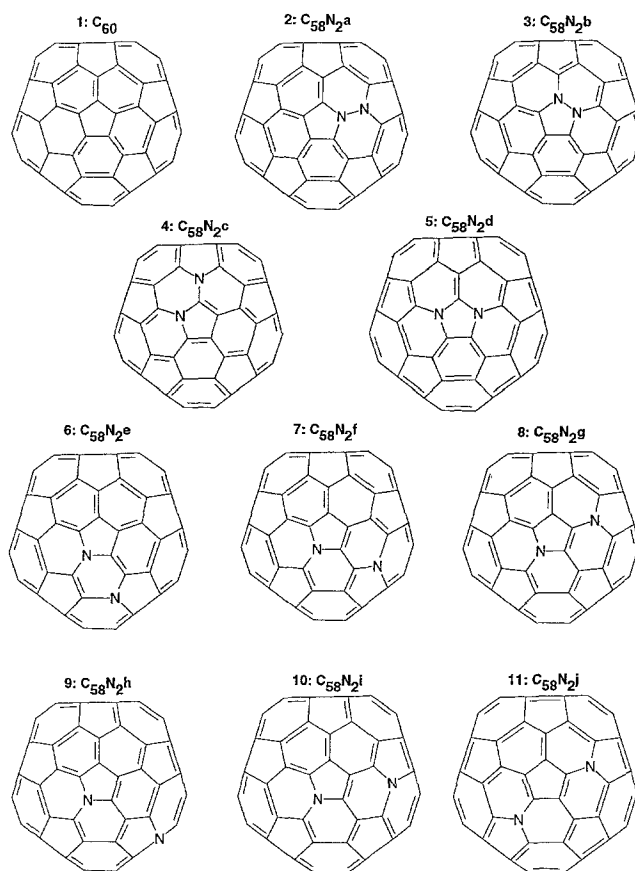

Fig. 1. The structures of C_{60} and some isomers of $C_{58}N_2$. The ten isomers correspond to entries 2 to 11 in Table 1.
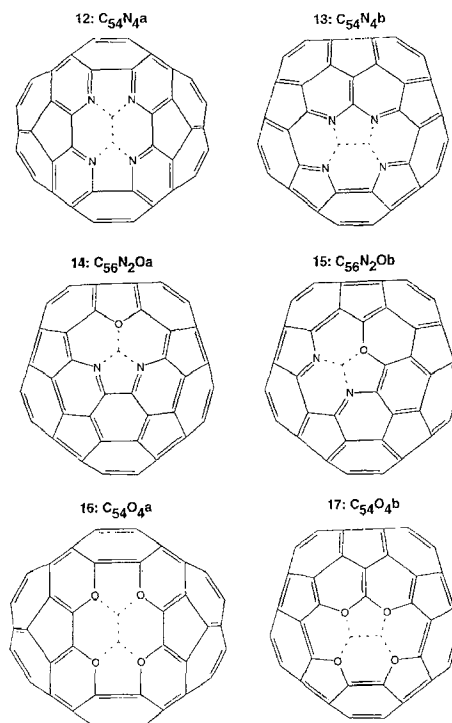
Fig. 2. The building principle of some 'truncated' heterofullerenes. Dashed lines indicate the vacancies or holes relative to the parent fullerene.

BUILDING PRINCIPLES

Heterofullerenes are derived from fullerenes by eliminating carbon atoms from the corresponding basic fullerene skeleton and by trying to fill the generated vacancies with heteroatoms. We will focus on ordinary closed shell systems. Two situations might arise from such a substitution process: either every eliminated carbon atom will be substituted by a heteroatom or, for valency or stability reasons, some vacancies cannot be filled by heteroatoms, thereby leading to spherical structures with holes. The two situations are shown in Figs. 1 and 2, respectively. We will term the second case as a 'truncated heterofullerene'.

For computational economy, we consider only heterofullerenes derived from C_{60} (molecule 1 in Fig. 1), but the same building principles could be applied to the higher fullerenes.

In Fig. 1, all the $C_{58}N_2$ topological isomers, where the shortest path between the two nitrogens consists of at most three carbons, are shown (structures 2 to 11). Some of these structures, e.g., structure 4, are optically active. The unfilled vacancies of some truncated heterofullerenes are indicated by dashed lines in Fig. 2. Structures 12 and 13 (or structures 16 and 17) are the two possible isomers of $C_{54}N_4$ (or $C_{54}O_4$) with touching vacancies. A faint resemblance to porphyrins or crown compounds should already be apparent at this point. Increasing the relative heteroatom content is straightforward and structures that are combinations of truncated and ordinary heterofullerenes are also conceivable. An extreme case of a truncated heterofullerene is given by the spherical $C_{24}N_{24}$ structure in Fig. 3, which is composed of eight s-triazine units. The macrocycles
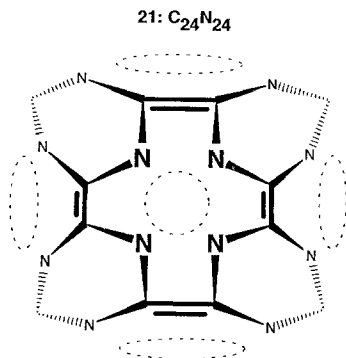
524

Fig. 3. A schematic presentation of the spherical $C_{24}N_{24}$ molecule. Dashed circles indicate the distorted macrocycles.

(each containing four nitrogens) are indicated by dashed circles. Other variants of truncated aza-fullerenes do exist in the reduced form and are discussed in detail below.

COMPUTATIONAL SECTION

Molecular modeling was performed with the CHARMM [13] and MACROMODEL [14] programs implemented on a Silicon Graphics 4D/25 workstation. Force-field calculations were done through the implementation of MM2 [15] and AMBER [16] in MACROMODEL. Semiempirical calculations were performed with the latest version of MOPAC 6.0 [17], implemented on an IBM-RS-6000/550 workstation. For the thermochemistry we used mainly the AM1 Hamiltonian [18] (and to some extent the PM3 Hamiltonian [19]). Some electronic properties (electrostatic potential-fitted charges [20], polarizabilities, etc.) were calculated, using the MNDO Hamiltonian at optimized AM1 geometry.

Semiempirical and ab initio calculations for fullerenes, usually for C_{60} and C_{70} under symmetry restrictions, have been published [21–26]. We encountered difficulties in optimizing the geometry of the presented molecules using internal coordinates. It turned out that the most efficient way to deal with such spherical molecules was to use Cartesian coordinates and the recently implemented eigenvector follower option (EF) of MOPAC 6.0. Using the high precision optimization option (i.e., the keyword PRECISE), the norm of the gradient at the energy minimum was usually below 0.01 kcal/mol/Angstrom.

To summarize the computational procedure: the molecules were modeled and geometry optimized with MACROMODEL. No problems with multiple minima were encountered with the MM2 or AMBER force fields, and the resulting optimized structures exhibited the expected symmetry (in contrast to geometry optimization with the CHARMM force field, which was rejected for that reason). The resulting structures were submitted to a full geometry optimization with MOPAC 6.0, using the XYZ and EF options.

It should be emphasized at this point that the aim of the calculation is not to produce absolute values of some observables. The emphasis is rather on the detection of trends in a series of consistent calculations.

RESULTS AND DISCUSSION

The results of the calculations for molecules **1** to **21** are summarized in Table 1. Structures **18** to **20** are not pictured and have the following meaning: Structure **18**, $C_{48}N_8$, corresponds to structure **12** with the same pattern (i.e., four nitrogens) on opposite sides of the sphere (i.e., two holes at the poles); structure **19**, $C_{48}N_4O_4$, is similar to structure **18** but contains the pattern of structure **16** (four oxygens) on opposite sides of the sphere. Finally, Structure **20**, $C_{36}N_{16}$, corresponds to structure **12** but with four 'four nitrogen' patterns arranged symmetrically about an axis (i.e., the 'four nitrogen' pattern is replicated at 90, 180 and 270 degrees) and can be considered as intermediate between structure **18**, $C_{48}N_8$, and structure **21**, $C_{24}N_{24}$.

The second column of Table 1 contains the AM1 and MNDO heats of formation. Both values refer to the AM1-optimized geometry. Of prime importance is the question about the reliability of these thermochemical data. A statistical analysis of the differences between the experimental and the calculated heats of formation [19] revealed that the root-mean-square deviation for a set of 276 C, H, N and O compounds is about 10, 18 and 8 kcal/mol for the AM1, MNDO and PM3 Hamiltonians, respectively. However, inside a generic family of compounds the error is usually an order of magnitude lower [26]. The third column of Table 1 (termed 'Strain') contains the MM2 and AMBER (total) energies (at the optimal geometry for these force fields). Refering to the stability ranking of the various isomers, the data in this column reveal the complete disagreement between MM2 and semiempirical quantum chemistry for these distorted π-systems (in contrast to the excellent correlation between the MNDO and AM1 results).

The first entry to Table 1 is C_{60} and the results are in full agreement with previously published results [24,25] and theory (e.g., the degeneracy of the HOMOs and LUMOs). Let us first discuss the results for the azafullerenes given in Fig. 1.

The first noteworthy fact is that out of the ten $C_{58}N_2$ isomers there is one of remarkable stability, structure **5**, with a heat of formation difference of about 15 kcal/mol from the next most stable isomer. Although not all isomers of $C_{58}N_2$ could be dealt with, there was nothing found which indicated that stability increased with increasing distance between the two nitrogens. The optimized geometries of the structures **2** to **11** are practically identical with the geometry of C_{60}, although the predicted vibrational spectra differ significantly as well as their electronic properties given by the HOMO and LUMO values. In spite of the small dipole moment of structure **5**, it does not differ electrostatically from C_{60}. The polarizabilities of the isomers (as well as C_{60}) are small and of the same order of magnitude. For comparative purposes we give the corresponding figures for a bisubstituted stilbene (hydroxy and nitro groups at opposing ends) considered as a candidate for the design of materials exhibiting non-linear optical properties (units and computational conditions as in Table 1): average polarizability = 6.6; second-order polarizability along dipole = 24.6; average third-onder polarizability = 136.6.

Turning to the truncated heterofullerenes (structures **12** to **21** in Table 1), it is seen that the more symmetrical structures are also the more stable ones (e.g., structure **12** is about 30 kcal/mol more stable than structure **13**). The optimized geometries of the truncated heterofullerenes in the vicinity of the aperture are distorted (when compared with C_{60}). The four nitrogen atoms of structure **12** define a rectangle with a short side of 2.71 Å and a long side of 2.91 Å. The values between the corresponding positions in C_{60} are 2.37 and 2.85 Å, respectively. In the extreme case of structure **21**, $C_{24}N_{24}$, which possesses a D_{4h} symmetry, the corresponding N-N distance is 2.71 Å.

TABLE 1
CALCULATED THERMOCHEMICAL AND ELECTRONIC PROPERTIES OF SOME HETEROFULLERENES

Molecule	HOF[a] AM1/ MNDO	Strain[b] MM2/ AMBER	HOMO 1–3 AM1	LUMO 1–3 AM1	Dipol[c] AM1/ MNDO	Av.[d] Charg. MNDO	Polar.[e] MNDO	Hyper-polar.[f] MNDO	Av.[g] gamma MNDO	Few most[h] intense vibrat.
1: C$_{60}$	973.4 879.7	1270 3845	−9.64 −9.64 −9.64	−2.95 −2.95 −2.95	0.0 0.0	0.0	1.57	0.00	29.2	573, 775, 1404, <u>1753</u>
2: C$_{58}$N$_2$a	1016.5 897.8	----[i] 3725	−9.30 −9.74 −9.76	−2.88 −3.04 −3.11	1.9 2.2	−0.17	1.57	−2.26	31.7	567, 1408, 1712, <u>1755</u>, 1781, 1823
3: C$_{58}$N$_2$b	1030.9 914.9	----[i] 3746	−8.91 −9.73 −9.77	−2.98 −3.08 −3.24	2.1 2.4	−0.09	1.59	−2.35	34.5	452, 704, 1410, 1642, <u>1743</u>, 1784
4: C$_{58}$N$_2$c	1023.8 905.4	1431 3791	−8.10 −9.64 −9.74	−2.75 −3.11 −3.24	0.64 0.88	+0.15	1.65	−6.26	55.5	342, 1296, 1599, 1658, 1713, <u>1751</u>
5: C$_{58}$N$_2$d	1002.9 887.4	1346 3668	−8.86 −9.72 −9.75	−2.78 −3.06 −3.10	1.58 1.87	+0.03	1.58	−3.76	35.4	751, 1279, 1405, 1540, <u>1738</u>, 1781
6: C$_{58}$N$_2$e	1019.0 901.0	1393 3726	−8.29 −9.68 −9.76	−2.73 −3.09 −3.30	1.12 1.33	+0.23	1.62	−4.94	42.6	347, 750, 1297, <u>1560</u>, 1591, 1740
7: C$_{58}$N$_2$f	1025.1 908.7	1401 3851	−8.14 −9.67 −9.74	−2.75 −3.13 −3.29	0.90 1.01	+0.56	1.65	−10.2	48.5	679, <u>1249</u>, 1370, 1562, 1615, 1735
8: C$_{58}$N$_2$g	1035.4 917.2	1358 3684	−7.82 −9.57 −9.72	−2.78 −3.13 −3.53	2.73 2.59	+0.54	1.73	−36.5	70.0	247, <u>1153</u>, 1200, 1288, 1358, 1600
9: C$_{58}$N$_2$h	1026.7 907.5	1318 3700	−8.04 −9.58 −9.74	−2.81 −3.03 −3.35	1.34 1.41	+0.36	1.67	−5.93	49.0	703, 1355, 1427, 1554, <u>1630</u>, 1708
10: C$_{58}$N$_2$i	1028.1 912.0	1368 3672	−7.82 −9.63 −9.67	−2.97 −3.06 −3.42	1.36 1.44	+0.53	1.74	−12.4	−17.2	252, 321, <u>1058</u>, 1554, 1594, 1703
11: C$_{58}$N$_2$j	1025.2 907.3	1381 3666	−8.04 −9.53 −9.70	−2.80 −3.05 −3.50	2.20 2.35	+0.47	1.65	−5.80	43.8	344, 710, 1443, 1544, <u>1620</u>, 1740
12: C$_{54}$N$_4$a	978.0 869.2	1496 3307	−9.71 −9.77 −9.82	−2.91 −3.05 −3.16	3.16 4.08	−0.50	1.53	−0.42	30.8	573, 1272, 1391, 1434, 1728, <u>1754</u>
13: C$_{54}$N$_4$b	1010.9 887.8	1265 3439	−9.67 −9.77 −9.83	−2.96 −3.12 −3.37	3.57 4.61	−0.52	1.52	−0.48	32.1	890, 1341, 1414, 1718, <u>1738</u>, 1764
14: C$_{56}$N$_2$Oa	942.5 813.3	1285 3453	−9.49 −9.69 −9.75	−2.82 −3.00 −3.11	1.93 2.73	N: −0.51 O: −0.38	1.55	−1.15	31.0	1125, 1246, 1412, 1728, <u>1749</u>, 1779
15: C$_{56}$N$_2$Ob	962.1 844.6	1241 3514	−9.29 −9.73 −9.76	−2.89 −3.09 −3.27	2.5 3.10	N: −0.56 O: −0.12	1.56	−1.01	33.2	1410, 1638, 1677, 1712, <u>1735</u>, 1770

TABLE 1 (continued)

Molecule	HOF[a] AM1/ MNDO	Strain[b] MM2/ AMBER	HOMO 1–3 AM1	LUMO 1–3 AM1	Dipol[c] AM1/ MNDO	Av.[d] Charg. MNDO	Polar.[e] MNDO	Hyper- polar.[f] MNDO	Av.[g] gamma MNDO	Few most[h] intense vibrat.
16:	807.4	1128	−9.34	−2.75	2.19	−0.14	1.52	−2.80	33.8	695, 1392,
$C_{54}O_4a$	678.5	3319	−9.47	−3.11	3.51					1494, 1565,
			−9.71	−3.13						1677, 1726
17:	833.1	1214	−8.02	−2.72	2.27	−0.25	1.68	−22.6	39.3	1159, 1252,
$C_{54}O_4b$	703.4	3330	−9.45	−2.90	2.05					1283, 1393,
			−9.69	−3.73						1536, 1637
18:	984.0	1730	−9.79	−2.70	0.01	−0.50	1.48	−0.1	32.1	827, 1210,
$C_{48}N_8$	860.2	2776	−9.90	−3.15	0.01					1389, 1633,
			−10.00	−3.38						1738, 1778
19:	813.1	1355	−9.51	−2.82	0.92	N: −0.55	1.47	2.71	35.9	1310, 1451,
$C_{48}N_4O_4$	669.6	2784	−9.76	−3.13	0.49	O: −0.12				1496, 1589,
			−9.89	−3.33						1676, 1701
20:	1001.0	1964	−9.89	−2.93	0.04	−0.65	1.38	0.03	35.4	843, 1418,
$C_{36}N_{16}$	821.1	1758	−10.63	−2.92	0.05					1489, 1622,
			−10.86	−3.72						1758, 1777
21:	1063.5	1787	−11.59	−2.85	0.00	−0.82	1.20	0.00	19.2	729, 839,
$C_{24}N_{24}$	796.0	369	−11.59	−3.02	0.00					1103, 1426,
			−11.70	−3.02						1659

[a] Heats of formation in kcal/mol. All MNDO results at AM1 equilibrium geometry.

[b] Energies in kj/mol after full minimization with MACROMODEL. 'Strain' is defined as the sum of energy contributions from bond streching, angle bending, torsion and non-bonded van der Waals and electrostatic interactions.

[c] Dipole moments in Debye.

[d] Average electrostatic potential fitted point charges on the heteroatoms (with scaling).

[e] Average polarizability in ESU*10^{-22}. All Calculations based on HOF (E4 in MOPAC 6.0 terminology).

[f] Second-order polarizability (beta) along the molecular dipole moment in ESU*10^{-30}.

[g] Average third-order polarizability (gamma) in ESU*10^{-36}.

[h] AM1 vibrational frequencies in cm^{-1}.

[i] No MM2 force-field parameters were available.

These N-N distances are amazingly close to the corresponding distance in phthalocyanine, that is (under the same computational conditions) 2.80 Å. The computed point charges on the nitrogen atoms of the truncated heterofullerene are slightly lower than the corresponding point charge of phthalocyanine (−0.70 under the same computational conditions). The higher symmetry of $C_{24}N_{24}$ is not only reflected in the degeneracy of the HOMOs and LUMOs but also in the vibrational spectrum, where now only five bands of significant intensity are predicted.

Some crude estimates on the incremental heat of formation per atom are given in the synthesis section below. The relatively high heats of formation of azafullerenes as compared with fullerenes should be advantageous in reactions leading to the destruction of the sphere, e.g., in diamond synthesis (see summary and conclusions below).

REDUCED TRUNCATED FULLERENES

Phthalocyanines and related compounds are known to exist in the doubly reduced form. In the

case of a truncated heterofullerene like structure **12**, $C_{54}N_4$, three different doubly reduced forms are obvious and are shown in Fig. 4, structures **22** to **24**. The corresponding AM1 heats of formation are given in parentheses. The outcome of the calculations indicates that the non-symmetric structure **24**, with the hydrogens located on the long side of the rectangle, is absolutely dominant and exceeds the symmetric structure **22** by almost 30 kcal/mol. In contrast to the phthalocyanines, the peculiar geometry of the truncated heterofullerene also allows for the four-fold reduced form. We started the AM1 geometry optimization from the obvious structure **25**. The outcome of the calculation was astonishing: this structure has no minimum in its vicinity and it relaxes to the unexpected structure **26** of Fig. 4, where one hydrogen has flipped out of the plane defined by the remaining three. The same result is reproduced when the PM3 instead of the AM1 Hamiltonian is used. This result immediately suggests that there exists an additional doubly reduced isomer shown as structure **27**. This 'kinked' geometry of $C_{54}N_4H_2$ is indeed stable and rather close in energy to the symmetrical structure **22**. On the other hand, the hydrocarbon analogue of structure **25**, where the nitrogen atoms are re-substituted by carbon atoms, i.e., $C_{58}H_4$, does not show this unusual flipping of one hydrogen atom.

Another outcome, which is as relevant, is the heat of hydrogenation. Structures **24** and **26** have practically the same heats of formation, which means that, from the thermochemical point of view, $C_{54}N_4H_2 + H_2$ is predicted to be in equilibrium with $C_{54}N_4H_4$.

Structure **21**, $C_{24}N_{24}$, at the extreme end of the truncated heterofullerene series, should be a 'hydrogen sponge', according to the last results. The AM1 heat of formation of $C_{24}N_{24}H_{24}$ is around 547 kcal/mol and it is in fact a mixture of dozens of isomers differing in the relative orientation of the asymmetric arrangements of the hydrogens around the hole. The energy difference between these different isomers is extremely small. We close this section by mentioning a possible application for solids composed of $C_{24}N_{24}H_{24}$-type molecules. These molecules exist in many easily con-
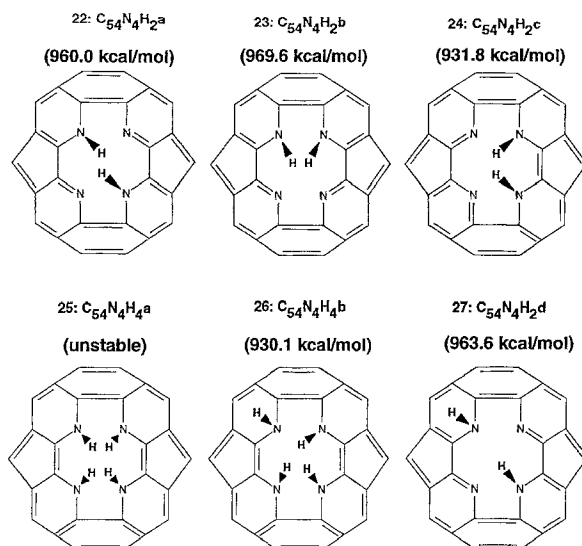

Fig. 4. A schematic representation of the geometry of the hydrogenated isomers of $C_{54}N_4$. The AM1 heats of formation are given in parentheses.

vertible isomers of almost identical energy and spectral properties, and may therefore be useful in persistent spectral hole burning [27,28].

SYNTHESIS PROPOSALS

The synthesis of fullerenes is conceptually rather simple and consists of vaporizing graphite by means of a laser beam or an electrical torch and then 'cooling' the vapor in a stream of helium. The yield of the resulting fullerenes is critically dependent on the pressure of the He atmosphere. Experiments where the He has been 'diluted' with other gases like NO, SO_2, CO NH_3 etc. are known [29,30]. The higher fullerenes (i.e., C_{60} and above) are either inactive toward these 'contaminations' or will add these contaminations to form substituted fullerenes, although hetero-atoms will usually not be incorporated into the basic skeleton. Three conditions are necessary for the incorporation of heteroatoms: the entity to be incorporated should have a sufficiently high heat of formation in order to be able to compete (in the thermodynamic sense) with small carbon clusters; it should fit into the mechanism of fullerene formation; and it should start to interact with the carbon clusters at a sufficiently early stage of fullerene formation. We believe that cyano-gen, C_2N_2, is a promising candidate for the following reasons.

Although the conditions prevailing during fullerene production are far from equilibrium and thus exclude a reliable thermochemical approach, some crude arguments in favor of heterofulle-rence production based on the thermochemical results achieved so far are given.

The average AM1 heat of formation per C atom in C_{60} is about 16.22 kcal/mol. The crudest assumption consists in assuming additivity per atom for the heterofullerenes, using the carbon increments from the parent fullerene. Using the results in Table 1, one can easily deduce that the average heat of formation per nitrogen in $C_{58}N_2$, i.e., in structure 5, is 31 kcal/mol and the average heats of formation per nitrogen in structures 12, 18 and 20 are all about 26 kcal/mol. These values might be too high for a successful synthesis using He/N_2 mixtures. Apart from its flammability and extreme toxicity, $(CN)_2$ has the pleasant property of possessing a high heat of formation. The AM1 heat of formation of this compound is about 68 kcal/mol and this brings us, at least thermochemically, close to predicted heats of formation of the heterofullerenes (e.g., $C_{56} + C_2N_2$ produces a heat of formation of 976 kcal/mol, not too far from 1002 kcal/mol, the heat of formation of structure 5).

The main reason for using cyanogen lies, however, in its known reactivity in the gas phase under plasma conditions [31,32], and its linear structure which is consistent with some ideas about the mechanism of fullerene formation [33], where linear carbon chains appear to link together to form graphitic sheets.

Cyanogen is formed upon heating metal cyanides like $Hg(CN)_2$ or AgCN. Using a graphite/cyanide composite target rod instead of pure graphite in an ordinary fullerene synthesis would allow an interaction between the cyanogen and carbon clusters or linear chains at an early stage of the fullerene formation.

BEHAVIOR TOWARDS ION PENETRATION

Fullerenes combine with alkali metals, and the best known representatives are the superconducting materials with the composition M_3C_{60} [9]. Although there is enough room inside the ful-
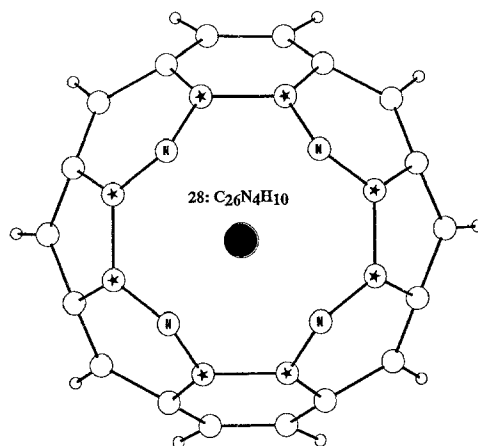
530

Fig. 5. A simplified model system for studying ion penetration and complexation reactions. The $C_{26}N_4H_{10}$ structure is forced to adopt the geometry of $C_{54}N_4$ by fixing the coordinates of the atoms shown as unfilled circles.

lerene molecule, the metal atoms will usually reside outside the fullerene sphere. Metals inside fullerenes, termed M@C$_{60}$, are known [12], with M usually being La, e.g., La@C$_{82}$ [34]. In the following we investigated the possibility of combining heterofullerenes with cations and anions and the energy profile of the penetration of ions into truncated heterofullerenes. The underlying models are very qualitative and electrostatic in nature, i.e., ions are presented by point charges with 'repulsion spheres' ('sparkles' in the terminology of MOPAC [17] have a vanishing heat of atomization, no orbitals and no ionization potential).

The first calculations were performed on the truncated heterofullerene $C_{48}N_8$, i.e., structure **18** in Table 1, combined with a cation or an anion. The resulting complexes were $C_{48}N_8M^+$ and $C_{48}N_8M^-$, where M designates the ion. The total number of valence electrons was the same in all complexes (i.e., 232 valuence electrons). M was positioned at different locations and the geometry of the system was then optimized. It turned out that the energy of an ion (cation as well as anion) was larger at the center of the sphere (which corresponds to a unique minimum) than outside the sphere. The AM1 energy difference between the system with an ion at the sphere center and the system with an ion outside the sphere was 148 kcal/mol in the case of $C_{48}N_8M^+$ and only 51 kcal/mol in the case of $C_{48}N_8M^-$. This result is somehow surprising: it suggests that fullerenes strongly prefer anions inside the sphere. In other words, fullerenes behave like microscopic Faraday cages where the mobile electron cloud repels itself and thus causes a positive electrostatic potential inside the sphere. Wrapping an anion in the fullerene envelope should be easier than wrapping a cation. It should be emphasized that this somehow surprising result is based on a purely electrostatic model which might apply to ions like Na$^+$ or K$^+$. The existence of various La@fullerenes means that higher-order effects must be taken into account when dealing with more complex ions.

To study the reaction coordinate of ion penetration into the truncated heterofullerene, we used the model compound **28**, $C_{26}N_4H_{10}$, shown in Fig. 5. Its geometry is derived from structure **12**, $C_{54}N_4$, by fixing the relative positions of the outer carbon atoms to those in $C_{54}N_4$. The added hydrogens were also kept fixed so that the geometry of the inner atoms was kept, as far as possible, to that of $C_{54}N_4$. The reaction coordinate is a line perpendicular to the plane defined by the four nitrogen atoms and passing through the center of the molecule.
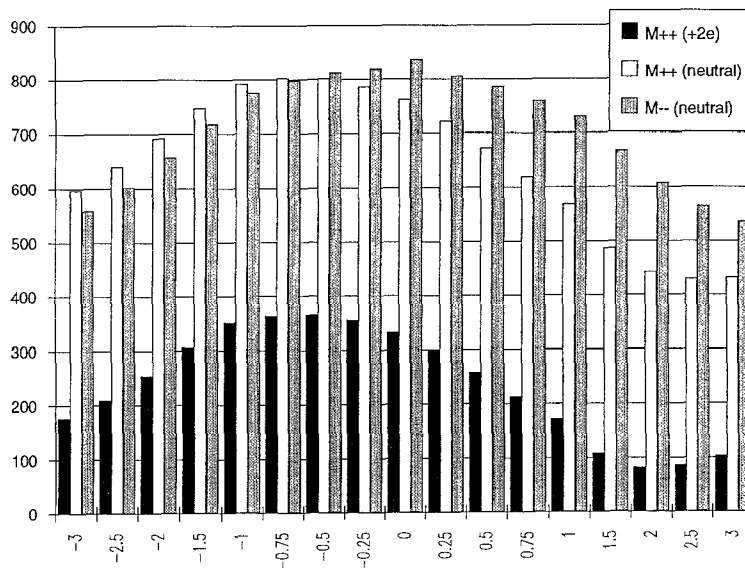
Fig. 6. The AM1 reaction coordinate for cation and anion penetration through the center of the model compound $C_{26}N_4H_{10}$ (structure **28**. Fig. 5). The bar heights are given in kcal/mol. The reaction coordinate is the distance from the center of the plane defined by the four nitrogens. A positive distance refers to the outer side of the hemisphere. The black bars refer to the case where two additional valence electrons have been added to the system.

The resulting calculations for the reaction coordinate are shown in Fig. 6. The black bars refer to the case where two electrons have been added to structure **28** (i.e., 136 valence electrons), the remaining bars refer to the case where no electrons have been added to the system (i.e., 134 valence electrons). The barriers for the penetration of ions are in all cases rather high, but one should not attach too much importance to these absolute values (the large heats of formation for these systems result from the enormous strain imposed on structure **28** and from the addition of hydrogens). More relevant is the fact that anions are more likely to penetrate into a heterofullerene than cations.

ASSEMBLAGE OF TRUNCATED HETEROFULLERENES

Phthalocyanines and related molecules currently belong to the most important molecular constituents of many novel and unconventional materials. Excellent reviews summarizing their uses as organic conductors, semiconductors, photoconductors, liquid crystals, Langmuir–Blodgett film materials, etc., have been published [35–38]. The 'active center' of phthalocyanines consists of four aromatic nitrogen atoms residing in a plane. We have already mentioned the remarkable geometrical and electrostatic similarity between this 'active center' and the four nitrogens of a truncated heterofullerene surrounding a common hole. Much effort has been invested in achieving conducting and semiconducting polymers by bridging the active centers of phthalocyanines with various ligands, predominantly transition metals and biaxial linking ligands [38,39]. Due to their curved shape and the possibility of several π-connected 'active centers' on one molecule, truncated heterofullerenes may offer many advantages over phthalocyanines for opening an electronic path-
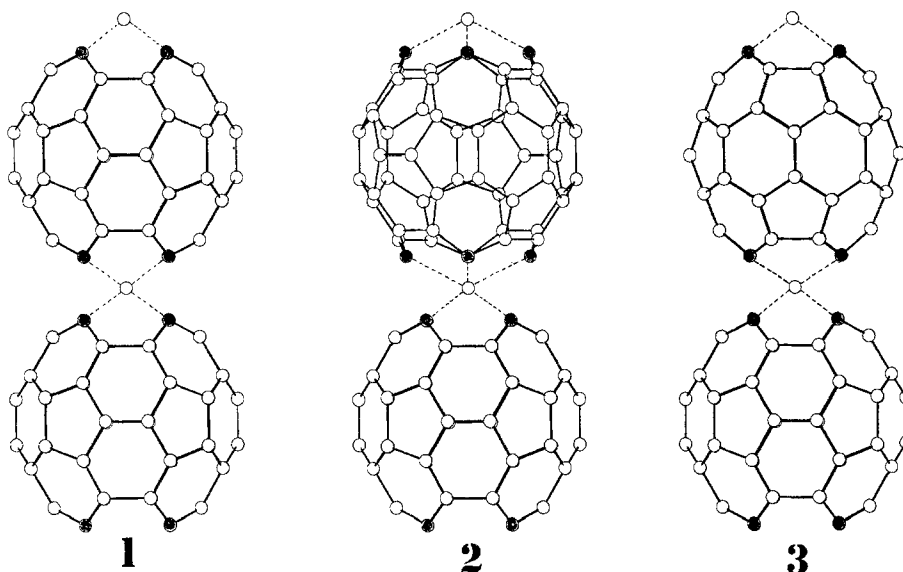
Fig. 7. The stacking of truncated heterofullerenes with two holes at opposing poles and metal atoms in between. The truncated heterofullerene shown corresponds to a side view of structure **18** (a top view would look like that of structure **12** in Fig. 2). 1 refers to the symmetric arrangement, 2 refers to the twisted arrangement, and 3 refers to the perpendicular arrangement. The heteroatoms are represented by solid circles.

way along the polymer axis. Although bridging of heterofullerenes in two and three dimensions is conceivable, we focus on the simple one-dimensional case depicted in Fig. 7, where the truncated heterofullerene $C_{48}N_8$ is considered. The rectangular structure of the four nitrogens makes three arrangements possible: the symmetric arrangement (**1** in Fig. 7), the twisted arrangement (**2** in Fig. 7), and the perpendicular arrangement (**3** in Fig. 7), where the long side of one rectangle is perpendicular to the short side on the other rectangle.

We used model systems for the MOPAC calculations because the size of such complexes is pro-
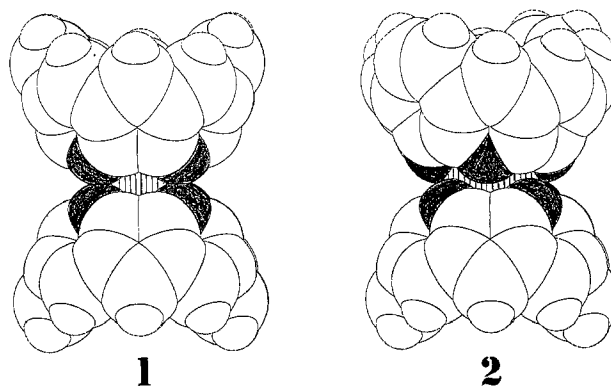

Fig. 8. The model system for estimating the geometry and energetics of the heterofullerene assemblages with a metal atom between the two distorted macrocycles. The ligands consist of the model structure $C_{26}N_4H_{10}$ shown in Fig. 5. Shown are the symmetrical and twisted sandwiches.

hibitive (we used the PM3 Hamiltonian for parametrization reasons). The calculations were designed to give some qualitative idea of this, as yet unknown, geometrical arrangement of atoms. We used structure **28** (Fig. 5) with fixed internal coordinates instead of $C_{48}N_8$. The resulting systems in the twisted and symmetrical arrangement are shown in Fig. 8, with a metal atom positioned between the two planes such that a sandwich-like complex emerges.

The PM3 results with M = Mg, Zn, Hg and Pb are summarized in Table 2. The first entry refers to the isolated $C_{26}N_4H_{10}$ molecule. The remaining entries consist of sub-tables for each metal atom. The 'single ligand' entry refers to the 1:1 complex between the metal and $C_{26}N_4H_{10}$. The only optimized geometric parameter is the distance from the metal atom to the planes defined by the four nitrogen atoms.

The relative stability of a sandwich complex consists of the difference between its energy and the sum of the 'single ligand' energy and the isolated $C_{26}H_4H_{10}$ energy. Thus, the Mg and Zn sandwiches are predicted to be very unstable, the Hg sandwich moderately unstable, and the Pb sandwich stable. Of course, only the ranking should be considered here as relevant. The twisted sandwich is predicted to be always the more stable arrangement. The band gap is the most important quantity in conjunction with conductivity discussions, but crystal orbital calculations for the systems shown in Fig. 7 are beyond our computational capabilities. The HOMO-LUMO deferences reported in Table 2 should be considered as a crude indicator of a trend. A significant drop in the

TABLE 2
PM3 RESULTS FOR SOME $(C_{26}N_4H_{10})_2M$ SANDWICH MODELS

M	Type[a]	PM3-HOF kcal/mol	Distance[b] M-plane	LUMO-[c] HOMO	Mull.[d] chg.M	Mull.[d] chg. N
	$Co_6N_4H_{10}$	419.4		3.6		+0.05
Mg	single ligand	349.5	0.00	5.2	+0.42	+0.12
	symmetric	824.3	1.47	2.2	+0.62	+0.08
	twisted	821.2	1.45	2.2	+0.61	+0.08
	perpendicular	824.7	1.47	2.2	+0.62	+0.08
Zn	single ligand	418.1	0.80	4.9	+0.23	+0.16
	symmetric	864.5	1.43	2.2	+0.21	+0.14
	twisted	858.6	1.38	2.2	+0.16	+0.14
	perpendicular	864.6	1.43	2.2	+0.21	+0.13
Hg	single ligand	368.2	0.67	5.4	+0.68	+0.06
	symmetric	781.2	1.43	2.2	+0.69	+0.07
	twisted	776.4	1.38	2.2	+0.67	+0.07
	perpendicular	781.6	1.44	2.2	+0.69	+0.07
Pb	single ligand	385.2	1.43	4.8	+0.65	+0.04
	symmetric	809.1	1.95	1.9	+0.89	+0.03
	twisted	808.9	1.94	1.9	+0.89	+0.02
	perpendicular	808.9	1.95	1.9	+0.89	+0.03

[a] 'Single ligand' refers to the $C_{26}N_4H_{10}M$ 1:1 complex. Symmetric, twisted and perpendicular refer to the sandwich complexes.

[b] The distance between the central atom and the plane defined by the four nitrogens.

[c] The energy gap in eV.

[d] Net atomic charges on M and nitrogen from the Mulliken population analysis.

HOMO/LUMO gap is indicated and the small gap in the case of the Pb sandwich should encourage the use of very large central atoms (i.e., lanthanides and actinides) for achieving high conductivity values.

Since transition metals as central atoms are of particular interest, it is tempting to treat such systems with ab initio methods. Ab initio GAUSSIAN calculations on simplified model compounds consisting of $C_8N_4H_8$ sandwiches, i.e., the innermost ring in structure **28** in the C_{4v} symmetry, are in progress.

CONCLUSIONS

It has been shown that two stable classes of heterofullerenes are possible: ordinary heterofullerenes, which are geometrically almost identical to the parent fullerenes, and 'truncated heterofullerenes', containing holes in the sphere.

The structural diversity is enormous and already begins at the level of heterofullerenes derived from C_{60}. Semiepirical AM1 and PM3 calculations were used to predict the properties of some representative molecules and revealed that there are clear thermochemical preferences for a limited number of isomers.

With regard to the potential uses of ordinary heterofullerenes, chemical reactions involving fullerenes [7,8] should also be possible with ordinary heterofullerenes. The geometrical and electrostatic similarity to the parent fullerenes should make these molecules ideal for adding to fullerene materials and thus enabling a tuning of the unusual properties of such materials. The crushing of C_{60} to diamond at room temperature and pressures over 20 GPa has recently been achieved [40]. We are confident that a similar procedure with heterofullerenes will lead to diamond (and small amounts of N_2) at much lower pressures.

With regard to the potential uses of truncated heterofullerenes, in addition to some of the uses mentioned above, truncated heterofullerenes are predicted to exist in various reduced forms. Truncated azafullerenes are predicted to be easily reducible. An unexpected an unusual geometry of the four-fold hydrogenated form is predicted to lead to a large number of easily inter-convertible, geometrically and spectrally almost identical isomers. Solids composed of such molecules could be of interest for persistent spectral hole burning. The remarkable geometrical similarity of the heteroatom arrangement about the hole compared with that in phthalocyanines and related compounds makes the use of truncated heterofullerenes feasible in all areas where phthalocyanines play a role. The possibility of combining in one rigid molecule several π-bridged macrocycles pointing in different directions is one of the main advantages offered by this class of molecules.

It was also shown that fullerenes in general resemble Faraday cages, where the mobile electrons concentrate on the outer side of the sphere, thereby creating a positive potential at the center of the sphere. This makes the wrapping of a cation in the fullerene envelope less probable than that of an anion.

Finally, a synthetic route to azalfullerenes was proposed. The simplest route consists of using mixtures of helium and cyanogen, $(CN)_2$, instead of pure helium in cooling the carbon vapors in a conventional fullerene synthesis. We believe that the most promising route is the simultaneous generation of cyanogen from cyanates like $Hg(CN)_2$ or $AgCN$ during the evaporation of carbon.

REFERENCES

1 Kroto, H.W., Heath, J.R., O'Brien, S.C., Curl, R.F. and Smalley, R.E., Nature, 318 (1985) 162.

2 Kroto, H.W., Allaf, A.W. and Balm, S.P., Chem. Rev., 91 (1991) 1213.

3 Haddon, R.C., Hebard, A.F., Rosseinsky, M.J., Murphy, D.W., Duclos, S.J., Lyons, K.B., Miller, B., Rosamilia, J.M., Fleming, R.M., Kortan, A.R., Glarum, S.H., Makhija, A.V., Muller, A.J., Eick, R.H., Zahurak, S.M., Tycko, R., Dabbagh, G. and Thiel, F.A., Nature, 350 (1991) 320.

4 Kochanski, G.P., Hebard, A.F., Haddon, R.C. and Fiory, A.T., Science, 255 (1992) 184.

5 Hebard, A.F., Rosseinsky, M.J., Haddon, R.C., Murphy, D.W., Glarum, S.H., Palstra, T.T.M., Ramirez, A.P. and Kortan, A.R., Nature, 350 (1991) 600.

6 Hirsch, A., Soi, A. and Karfunkel, H.R., Angew. Chem., 104 (1992) 808.

7 Suzuki, T., Li, Q., Khemani, K.C., Wudl, F. and Almarsson, O., Science, 254 (1991) 1186.

8 Krusic, P.J., Waserman, E., Keizer, P.N., Morton, J.R. and Preston, K.F., Science, 254 (1991) 1183.

9 Holczer, K., Klein, O., Huang, S-M., Kaner, R.B., Fu, K-J., Whetten, R.L. and Diederich, F., Science, 252 (1991) 1154.

10 Diederich, F., Whetten, R.L., Thilgen, C., Ettl, R., Chao, I. and Alvarez, M.M., Science, 254 (1991) 1768.

11 Ettl, R., Chao, I., Diederich, F. and Whetten, R.L., Nature, 353 (1991) 149.

12 Chai, Y., Guo, T., Jin, C., Haufler, R.E., Felipe Chibante, L.P., Fure, J., Wang, L., Alford, J.M. and Smally, R.E., J. Phys. Chem., 95 (1991) 7564.

13 Brunger, A.T., Brooks III, C.L. and Karplus, M., Proc. Natl. Acad. Sci. USA, 82 (1985) 8458.

14 Mohamadi, F., Richards, N.G.J., Guida, W.C., Liskamp, R., Lipton, M., Caufield, C., Chang, G., Hendrickson, T. and Still, W.C., J. Comp. Chem., 11 (1990) 440.

15 Burkert, U. and Allinger, N.L., Molecular Mechanics, ACS Monograph 177, American Chemical Society, Washington D.C., 1982.

16 Weiner, S.J., Kollman, P., Case, D., Singh, U., Ghio, C., Alagona, G., Profeta, S. and Weiner, P., J. Am. Chem. Soc., 106 (1984) 765.

17 Stewart, J.J.P., QCPE 1990, QCPE 455, MOPAC Version 6.0.

18 Dewar, M.J.S., Zoebisch, E.G., Healy, E.F. and Stewart, J.J.P., J. Am. Chem. Soc., 107 (1985) 3902.

19 Stewart, J.J.P., J. Comp. Chem., 10 (1989) 221.

20 Besler, B.H., Merz Jr., K.M. and Kollman, P.A., J. Comp. Chem., 11 (1990) 431.

21 Stanton, R.E., J. Phys. Chem., 96 (1992) 111.

22 Lüthi, H.P. and Almlöf, J., Chem. Phys. Lett., 135 (1987) 357.

23 Rudzinski, J.M., Slanina, Z., Togasi, M. and Osawa, E., Thermochimia Acta, 125 (1988) 155.

24 Slanina, Z.J., Rudzinski, J.M., Togasi, M. and Osawa, E., Mol. Struct. (Theochem), 202 (1989) 169.

25 Stewart, J.J.P. and Coolidge, M.B., J. Comp. Chem., 12 (1991) 1157.

26 Bakowies, D. and Thiel, W., J. Am. Chem. Soc., 113 (1991) 3704.

27 Moerner, W.E., In Persistent Spectral Hole-Burning: Science and Application, Topics in Current Physics, Volume 44, Springer-Verlag, Heidelberg, 1988.

28 Gorokhovskii, A.A., Kaarli, R.K. and Rebane, L.A., Opt. Commun., 16 (1976) 282.

29 Zhang, Q.L., O'Brien, S.C., Heath, J.R., Liu, Y., Curl, R.F., Kroto, H.W. and Smalley, R.E., J. Phys. Chem., 90 (1986) 525.

30 Sunderlin, L.S., Paulino, J.A., Chow, J., Kahr, B., Ben-Amotz, D. and Squires, R.R., J. Am. Chem. Soc., 113 (1991) 5489.

31 So, Y.H. and Miller, L.L., J. Am. Chem. Soc., 103 (1981) 4204.

32 Henis, N.B.H. and Miller, L.L., J. Am. Chem. Soc., 104 (1982) 2526.

33 Curl, R.F. and Smalley, R.E., Scientific Am., October 1991, 32.

34 Johnson, R.D., de Vries, M.S., Salem, J., Bethune, D.S. and Yannoni, C.S., Nature, 355 (1992) 239.

35 Schulz, H., Lehmann, H., Rein, M. and Hanack, M., Structure and Bonding, 74 (1991) 43.

36 Hanack, M., Chimia, 37 (1983) 238.

37 Hanack, M., Isr. J. Chem., 25 (1985) 205.

38 Münz, X. and Hanack, M., Chem. Ber., 121 (1988) 235.

39 Koch, W., Ph.D. Dissertation, University of Tübingen, 1986.

40 Regueiro, M.N., Monceau, P. and Hodeau, J-L., Nature, 355 (1992) 237.